



The interactive effects of ocean acidification and warming on bioeroding sponge *Sphaciospongia vesparium* microbiome indicated by metatranscriptomics

Guangjun Chai, Jinlong Li, Zhiyong Li^{*}

Marine Biotechnology Laboratory, State Key Laboratory of Microbial Metabolism and School of Life Sciences and Biotechnology, Shanghai Jiao Tong University, Shanghai 200240, China

ARTICLE INFO

Keywords:

Sphaciospongia vesparium
Metatranscriptomics
Ocean warming
Ocean acidification
Interactive effect

ABSTRACT

Global climate change will cause coral reefs decline and is expected to increase the reef erosion potential of bioeroding sponges. Microbial symbionts are essential for the overall fitness and survival of sponge holobionts in changing ocean environments. However, we rarely know about the impacts of ocean warming and acidification on bioeroding sponge microbiome. Here, the structural and functional changes of the bioeroding sponge *Sphaciospongia vesparium* microbiome, as well as its recovery potential, were investigated at the RNA level in a laboratory system simulating 32 °C and pH 7.7. Based on metatranscriptome analysis, acidification showed no significant impact, while warming or simultaneous warming and acidification disrupted the sponge microbiome. Warming caused microbial dysbiosis and recruited potentially opportunistic and pathogenic members of *Nesiotobacter*, *Oceanospirillaceae*, *Deltaproteobacteria*, *Epsilonproteobacteria*, *Bacteroidetes* and *Firmicutes*. Moreover, warming disrupted nutrient exchange and molecular interactions in the sponge holobiont, accompanied by stimulation of virulence activity and anaerobic metabolism including denitrification and dissimilatory reduction of nitrate and sulfate to promote sponge necrosis. Particularly, the interaction between acidification and warming alleviated the negative effects of warming and enhanced the *Rhodobacteraceae*-driven ethylmalonyl-CoA pathway and sulfur-oxidizing multienzyme system. The microbiome could not recover during the experiment period after warming or combined stress was removed. This study suggests that warming or combined warming and acidification will irreversibly destabilize the *S. vesparium* microbial community structure and function, and provides insight into the molecular mechanisms of the interactive effects of acidification and warming on the sponge microbiome.

1. Introduction

The current atmospheric carbon dioxide (CO₂) concentration has reached 410 parts per million (ppm), representing a 48% increase since pre-industrial times (before 1750) (WMO, 2020). As the planet's heat and anthropogenic CO₂ sinks, the ocean has absorbed the majority of the excess heat produced by the greenhouse, as well as approximately one-third of the anthropogenic CO₂, causing subsequent ocean warming and acidification (Hoegh-Guldberg and Bruno, 2010; Sabine et al., 2004). The Intergovernmental Panel on Climate Change (IPCC) has predicted that the mean surface temperature will rise 1.1–4.0 °C by the end of this century, accompanied by a further 0.3–0.5 unit decline in the surface ocean pH (IPCC, 2014). Physical and chemical changes in the

ocean have both direct and indirect effects on marine creatures' community balance and physiological processes, resulting in negative implications for coral reef ecosystems (Doney et al., 2012; Hoegh-Guldberg et al., 2007). Sponges, as important structural and functional components of benthic ecosystems, are generally more resistant to environmental changes than corals and have been proposed as potential winners under future global climate change (Bell et al., 2018; Bennett et al., 2017). However, our understanding of the impacts of future global climate change on sponge holobionts is still limited, particularly from the point of view of sponge microbiome since microbial symbionts are essential for marine macroorganisms' overall fitness and survival under environmental perturbations (Apprill, 2017; Bourne et al., 2016; Ugarelli et al., 2017).

^{*} Corresponding author.

E-mail address: zyli@sjtu.edu.cn (Z. Li).

<https://doi.org/10.1016/j.micres.2023.127542>

Received 3 August 2023; Received in revised form 30 October 2023; Accepted 1 November 2023

Available online 7 November 2023

0944-5013/© 2023 Elsevier GmbH. All rights reserved.

Sponges frequently harbor highly diverse and specific microbial symbionts (Thomas et al., 2016), which determine the trophic ecology of sponge holobionts (Lesser et al., 2022), contribute to microbiome-mediated functions such as chemical defense, and underpin the holobionts' stability and maintenance (Webster and Thomas, 2016). Generally, the consequences of climate change stressors for sponge microbiome are varied and sponge species-specific (Bell et al., 2018; Pita et al., 2018). For instance, some sponges remain stable microbial composition irrespective of elevated temperature (Lesser et al., 2016; Luter et al., 2020; Posadas et al., 2022; Ribeiro et al., 2020; Strand et al., 2017), whereas others experience microbial shift and decline in host health at high temperature (Fan et al., 2013; Luter et al., 2012), and even exhibit microbiome changes at temperatures lower than the thermal threshold that induces host bleaching or necrosis (Ramsby et al., 2018; Vargas et al., 2021).

Although growing studies have examined the effects of ocean warming or/and acidification on the microbial community structure of sponge holobionts (Fan et al., 2013; Kandler et al., 2018; Lesser et al., 2016; Luter et al., 2020; Luter et al., 2012; Morrow et al., 2015; Posadas et al., 2022; Ramsby et al., 2018; Ribeiro et al., 2020; Ribes et al., 2016; Strand et al., 2017; Vargas et al., 2021), few have investigated the functional profile change of sponge microbial symbionts. For instance, elevated temperature causes disruption of symbiotic interactions and induction of opportunistic scavengers in the *Rhopaloeide odorabile* holobiont (Fan et al., 2013), and induces microbial dysbiosis and nutrient cycling imbalance in *Stylissa flabelliformis* (Botté et al., 2023). The microbiome of *Coelocarteria singaporensis* could enhance metabolic capacity for energy-efficient carbon and nitrogen metabolism under acidification conditions at volcanic CO₂ seeps (Botté et al., 2019). Additionally, functional responses of the symbiotic communities under future climate scenarios have been assessed by functional profile prediction (Lesser et al., 2016; Morrow et al., 2015; Posadas et al., 2022). Since only a limited number of microbial symbiont genomes have been retrieved from multiple sponges (Engelberts et al., 2020), functional prediction currently has some restrictions and cannot accurately capture the functional profile of sponge microbiome. Meanwhile, few studies have considered the combined effects of ocean warming and acidification on sponge microbiome function (Bell et al., 2018), as well as the recovery potential of sponge microbiome after these stresses (Ramsby et al., 2018).

Bioeroding sponges can penetrate calcium carbonate substrates, and appear to be comparatively more resilient against environmental change than corals (Schönberg et al., 2017). The increased bioerosion potential by excavating sponges in future environmental scenarios presents a threat to coral reefs (Sacristán-Soriano et al., 2020). Thus, it is very essential to evaluate the impacts of ocean warming or/and acidification on bioerosion sponges. A previous investigation has assessed the effects of ocean warming on the microbiome of the ecologically important bioeroding sponge *Cliona orientalis* (Ramsby et al., 2018). However to date, little is known about the effects of ocean warming or/and acidification on the microbiome of bioeroding sponges. As a member of bioeroding sponges from the Clionidae family (Sacristán-Soriano et al., 2020) and a high microbial abundance species (Weisz et al., 2008), *Sphaciospongia vesparium* is widespread in coral reefs (Butler et al., 2018; He et al., 2014). *S. vesparium* provides structural habitat for other marine invertebrates (Butler et al., 1995), and actively uptakes the seawater dissolved organic carbon (Letourneau et al., 2020). Thus, understanding the response mechanism of *S. vesparium* under future global climate change scenarios is crucial for coral reef ecosystems. In this study, we sought to determine the response of the *S. vesparium* microbiome to ocean warming or/and acidification (32 °C or/and pH 7.7) in a laboratory simulation system. The structural and functional changes and recovery potential of the metabolically active microbial community of the bioeroding sponge *S. vesparium* were analyzed using metatranscriptomics.

2. Materials and methods

2.1. Sample collection and experimental design

Twenty individuals of sponge *S. vesparium* were collected by SCUBA at 8 m depth in Xuwen National Coral Reef Nature Reserve, the South China Sea (N20°15'29" E109°54'28"), October 2013. The nature reserve's annual mean SST is about 25 °C (Zhao et al., 2008). The sponge samples were cut into approximately 15 cm³ clones and transported to flow-through aquaria at the local reserve monitoring station for 7 days of acclimation. The same laboratory simulation system as described by Li et al. (2023) was used. The aquaria were maintained at 26 °C and pH 8.1 corresponding to the ambient environmental conditions at the time of collection. After acclimation, only healthy sponge samples were randomly distributed into twelve 100 L tanks, each with five sponge individuals, for the next simulation experiment based on predicted temperature and pH levels for 2100 (IPCC, 2014). The twelve tanks were randomly divided into four groups, each with three replicates: control (C, ambient pH 8.1 and temperature 26 °C), acidification (A, reduced pH 7.7 and ambient temperature 26 °C), warming (W, ambient pH 8.1 and elevated temperature 32 °C), and combined stress (AW, reduced pH 7.7 and elevated temperature 32 °C) (Fig. 1). Temperature levels were regulated by aquarium heaters (EHEIM, Germany). Elevated CO₂ concentrations were achieved by bubbling pure CO₂ and controlled by a pH controller (UP-aqua, China). The final elevated temperature and reduced pH were gradually reached during 3 days to minimize physiological shock caused by abrupt environmental changes. All tanks were filled with sand-filtered seawater at a flow rate of 30 L h⁻¹ using submerged pumps and illuminated with compact fluorescent tubes of 180–200 μmol quanta m⁻² s⁻¹ with 12:12 h diurnal cycle. Each tank's temperature, pH and salinity were monitored daily. Total alkalinity was measured using Orion™ Total Alkalinity Test Kit (Thermo Fisher Scientific, USA). Other carbonate parameters, such as partial pressure of carbon dioxide, calcite saturation and aragonite saturation, were calculated using the CO2SYS program (Pierrot et al., 2006). The seawater carbonate chemistry conditions of the stress-exposure groups were stable throughout the experiments (Table S1).

Before the stress exposure, the first sampling (hereinafter referred to as T0, n = 3) was taken randomly from the acclimated sponge samples. Sponge samples from groups W and AW showed signs of necrosis after 6 days of exposure to stress, thus the second sampling was taken from each group (one clone from each replicate tank, n = 3). The seawater temperature and pH were then gradually returned to the control levels for one day and were maintained to assess the recovery of sponge microbiome. The third sampling was operated after another 8 days (hereinafter referred to as 'P', n = 3 for each stress removal group) because no signs of recovery were observed in groups PW and PAW. All the samples were immediately cut and incubated in a 10-fold volume RNAlater (Dongsheng Biotech, China) and stored at – 80 °C.

2.2. Total RNA extraction and cDNA synthesis

Sponge samples were ground using a mortar and pestle in liquid nitrogen. Total RNA was extracted from a 500 mg homogenized sample using the RNeasy Plant Mini Kit (Qiagen, Germany) following the manufacturer's instructions. Genomic DNA was digested using RNase-free DNase (Qiagen, Germany). RNA samples were examined for DNA contamination using PCR and then quantified by an ND-1000 UV-Vis Spectrophotometer (Thermo Fisher Scientific, USA). Purified RNA was converted to cDNA using the SuperScript First-Strand Synthesis (Invitrogen, USA) protocol with random hexamers primer. cDNA samples were quantified using a Qubit 2.0 Fluorometer (Invitrogen, USA), and quality was checked on a 0.8% agarose gel. The resulting RNA and cDNA were stored at – 80 °C.

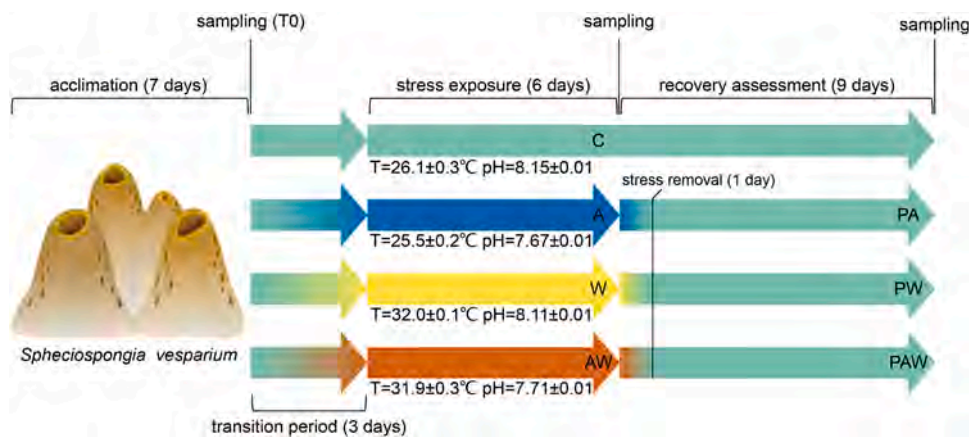


Fig. 1. Stress treatment and sampling procedure. T0, initial group before stress exposure; C, control; A, acidification; W, warming; AW, acidification and warming; P, stress removal group.

2.3. 16S rRNA amplicon sequencing and analysis

About 100 ng cDNA from each sample was used to construct a 16 S rRNA amplicon sequencing library by MetaVx™ Library Preparation kit (GENEWIZ, USA) at GENEWIZ (Suzhou, China). A panel of proprietary primers for relatively conserved regions bordering the V3, V4 and V5 hypervariable regions of prokaryotic 16 S rRNA gene were used to generate amplicons for taxonomic analysis. The V3 and V4 regions were amplified using forward primer “CCTACGRRBGCASCAGKVRVGAAT” and reverse primer “GGACTACNVGGGTWTCTAATCC”. The V4 and V5 regions were amplified using forward primer “GTGY-CAGCMGCCGCGGTAA” and reverse primer “CTTGTGCGGKCCCCCGY-CAATTC”. cDNA libraries were validated using the Agilent 2100 Bioanalyzer (Agilent Technologies, USA), and quantified by Qubit and real-time PCR (Applied Biosystems, USA). Paired-end sequencing (300 bp) was performed on the Illumina MiSeq platform (Illumina, USA).

The quality of the raw amplicon sequencing data was assessed with the FastQC program (<http://www.bioinformatics.babraham.ac.uk/projects/fastqc/>). Sequencing adaptors and poor-quality bases were trimmed using Trimmomatic v0.38 (Bolger et al., 2014) with default parameters. The resulting read pairs were merged using PANDAseq v2.8 (Masella et al., 2012). Merged reads with lengths longer than 470 bp or less than 425 bp, or that contained homopolymers exceeding 8 bp and ambiguous base calls, were removed. The remaining reads were then imported into QIIME2 v2021.2 (Bolyen et al., 2019). Dereplication and chimera filtering were performed using VSEARCH v2.7.0 (Rognes et al., 2016). Chimera free reads were clustered into operational taxonomic units (OTUs) with Greengenes 13.8 database at 97% identity (McDonald et al., 2012), using the vsearch cluster-features-open-reference plugin. A naive Bayes classifier (Bokulich et al., 2018) was trained on the Greengenes 13.8 97% OTUs database with reference sequences trimmed to the V3-V5 rRNA regions for taxonomic assignment. The OTU sequences were assigned based on the trained classifier using the feature-classifier plugin with classify-sklearn method (Pedregosa et al., 2011). OTUs classified as eukaryotes, mitochondria and chloroplasts were removed. A rooted phylogenetic tree was created with FastTree v2.1.10 (Price et al., 2010) using MAFFT alignment (Katoh and Standley, 2013). OTUs comprising less than 0.001% of total sequences or presenting in only one sample were removed (Bokulich et al., 2013).

2.4. Metatranscriptome sequencing and analysis

RNA sequencing library was constructed for each sample using a ribosomal RNA depletion strategy. Eukaryote or prokaryote rRNA was subtracted from the total RNA by Ribo-Zero rRNA removal kits

(Epicentre Biotechnologies, USA). The rRNA-depleted mRNA was then fragmented for library construction with an estimated mean insert size of 300 bp. Paired-end sequencing (125 bp) was performed on the Illumina HiSeq2500 platform (Illumina, USA).

The metatranscriptome reads were trimmed using Trimmomatic v0.38 (Bolger et al., 2014) with a minimum phred score of 25 and a minimum length of 75. Sequencing adaptors were removed and reads with ambiguous base calls were excluded. The remaining read pairs were merged by fastq-join v1.3.1 (<https://github.com/brwnj/fastq-join>) and were then submitted to the Metagenomics Rapid Annotation using Subsystems Technology (MG-RAST) server v3.0 (Meyer et al., 2008). Dereplication pipeline options were chosen to remove artificial replicate sequences produced by sequencing. The SEED subsystems and COG databases were utilized for functional annotation, and the Refseq database was used for taxonomic classification with default settings: e-value 10^{-5} , percent identity 60% and minimum alignment length of 15. Because no archaea sequences were detected by amplicon sequencing, only bacteria-related taxonomic and functional data were retrieved for further analysis.

3. Statistical analysis

OTU counts were rarefied to the minimum sequence depth ($n = 81,179$) retrieved from the samples. Alpha diversity indices including observed OTUs and Shannon H' were calculated using the core metric plugin. The normality and variance homogeneity of the indices were checked using Shapiro-Wilk and Levene's tests, respectively. Significant differences among groups were analyzed by one-way analysis of variance (ANOVA), followed by Tukey's honestly significant difference (HSD) post hoc tests using package agricolae v1.3.5 (<https://CRAN.R-project.org/package=agricolae>) in R software v4.0.2 (<http://www.r-project.org>). A two-way ANOVA with temperature and pH as factors was performed to detect the significance of differences in the alpha diversity indices under stress conditions.

For beta diversity estimation, the rarefied OTU table was square-root transformed, and a Bray-Curtis distance matrix (Bray and Curtis, 1957) was constructed. The functional annotation table for the metatranscriptome was standardized in order to generate a Hellinger distance matrix, which was then visualized using NMDS analysis to evaluate functional differences among groups. The significance of group separation was determined by permutational multivariate analysis of variance (PERMANOVA, using 999 permutations). Monte Carlo p values (999 permutations) were applied if pairwise comparisons resulted in insufficient unique permutations. A two-way PERMANOVA with temperature and pH as factors was performed to determine the significance of differences in the microbial community structure and function under stress

conditions. NMDS analysis and PERMANOVA were conducted in PRIMER v7 with the PERMANOVA+ add-on (PRIMER-e, Quest Research Limited, Auckland, NZ). Differentially abundant OTUs were identified using package DESeq2 v1.30.1 (Love et al., 2014) based on two criteria: (i) False Discovery Rate (FDR)-adjusted $P < 0.05$, and (ii) minimum relative abundances of 0.5% in at least two replicates of one group. Differentially expressed genes (DEGs) were defined as $\log_2|\text{fold change}| \geq 1$ and FDR-adjusted $P < 0.001$. Pairwise contrasts were computed for the final control C versus the initial T0 (C vs T0), each stress exposure group versus the final control (A vs C, W vs C, and AW vs C), and each stress removal group versus its corresponding stress exposure group (PA vs A, PW vs W, and PAW vs AW). Selected OTUs and DEGs were visualized using Cytoscape v3.6.1 (Shannon et al., 2003) and package pheatmap v1.0.12 (<https://CRAN.R-project.org/package=pheatmap>). Venn diagrams were constructed using package Vennrable v3.1.0.9000 (<https://github.com/js229/Vennerable>).

4. Results

4.1. RNA-level active microbial community structure change of sponge *S. vesparium* under and after warming or/and acidification

Using a laboratory system simulating ocean warming (32 °C) or/and acidification (pH 7.7) (Fig. 1), we analyzed the response of the *S. vesparium* microbiome based on metatranscriptome. A total of 3961,393 raw 16 S rRNA reads were generated from 24 samples (T0, C, A, W, AW, PA, PW and PAW, $n = 3$, respectively) by amplicon sequencing, with an average of $165,058 \pm 6418$ se. (standard error). Following quality filtering and noise reduction, 3001,998 high-quality 16 S rRNA reads with an average of $125,083 \pm 6081$ se. were obtained (Table S2a). After removing chimeric artifacts and contaminants, these sequences were clustered into 1362 OTUs with a 97% similarity threshold. Rarefaction curves for both observed OTUs and the Shannon index approached plateaus in all samples, indicating that the majority of microbial diversity had already been captured (Fig. S1). The overall microbial communities contained 12 bacterial phyla and one candidate division (Fig. 2a). The dominant phylum was *Proteobacteria*, ranging from 81% to 98%. Most of the proteobacterial OTUs were classified as *Alphaproteobacteria* (69% \pm 4% s.e.) and *Gammaproteobacteria* (20% \pm 2% s.e.).

The active microbial communities in the initial group T0 and the final control C exhibited high similarity (Fig. 2a), with similar Shannon H' (Fig. 2h) and observed OTU values (Fig. S2). They clustered together in the NMDS plot (PERMANOVA, $F = 0.83$, $P = 0.57$) (Fig. 2i) and no significantly changed OTUs were identified (Fig. 3a), indicating that the active microbial community composition in the control was stable, and thus the comparison between the stress-exposure groups and the control was feasible. The active microbial community of group C was dominated by *Alphaproteobacteria* (75.5%) and *Gammaproteobacteria* (22.2%) (Fig. 2a; Table S2b). Two dominant OTUs were unclassified *Alphaproteobacteria* OTU1 (70.2%) and unclassified *Gammaproteobacteria* OTU16 (20.3%), followed by unclassified *Alphaproteobacteria* OTU2 (0.7%) and OTU3 (0.6%) and EC214 OTU52 (0.7%), sharing high similarity to sponge or coral-derived symbionts (Table S2c).

The acidification group A was dominated by *Alphaproteobacteria* (64%) and *Gammaproteobacteria* (28%), similar to group C (Fig. 2a to c). The active microbial community composition in group A was not significantly changed (PERMANOVA, $F = 0.96$, $P = 0.45$) (Fig. 2i) and no differentially abundant OTUs were identified (Fig. 3b and c). Acidification had an insignificant effect on the Shannon index and microbial community structure, whereas the effects of warming and combined stress were significant (Table 1). Particularly, group W had the highest Shannon index ($H' = 4.8 \pm 0.04$ se.; Tukey's HSD, $P < 0.001$), followed by group AW ($H' = 3.1 \pm 0.18$ se.; $P = 0.016$) relative to group C ($H' = 1.8 \pm 0.1$ se.) (Fig. 2h).

The warming group W showed a significantly different microbial

community composition when compared with group C (PERMANOVA, $F = 3.45$, $P = 0.004$) (Fig. 2i). Unclassified *Alphaproteobacteria* (33.3%) and unclassified *Gammaproteobacteria* (8.4%) decreased significantly (Fig. 2b and c; Table S2b). Conversely, alphaproteobacterial family *Rhodobacteraceae* (23.8%) became dominant, accompanied with significantly increased gammaproteobacterial family *Oceanospirillaceae* (4%), deltaproteobacterial family *Desulfobacteraceae* (3.1%) and *Desulfovibrionaceae* (1.8%), epsilonproteobacterial family *Campylobacteraceae* (2.2%), *Bacteroidetes* family *Flammeovirgaceae* (5.5%) and *Cryomorphaceae* (2.2%), and *Firmicutes* family *Lachnospiraceae* (0.7%) and *Clostridiaceae* (0.4%) (Fig. 2b to g; Table S2b). Twenty-five differentially abundant OTUs were identified in group W, with 3 decreased and 22 increased (Fig. 3b and c; Table S2d). The 3 decreased OTUs (OTU2, OTU3 and OTU16) were members of the control's top abundant OTUs, especially the natively dominant *Gammaproteobacteria* OTU16 (0.2%) (Fig. 3f). Additionally, the natively most abundant *Alphaproteobacteria* OTU1 declined to 32.6% without significance ($P\text{-adjust} = 0.55$) (Fig. 3f; Table S2c). The most increased OTU was *Nesiotobacter* OTU6 (12.6%), followed by *Nautella* OTU7 (4.5%), *Gammaproteobacteria* OTU17 (4.3%), *Flammeovirgaceae* OTU41 (2.7%) and *Desulfobacteraceae* OTU31 (2.5%) (Fig. 3f; Table S2d). Notably, *Flammeovirgaceae* OTU41, *Desulfobacteraceae* OTU31, *Gammaproteobacteria* OTU18 (0.8%), *Desulfovibrio* OTU34 (0.8%) and *Arcobacter* OTU37 (1.4%) were closely matched to sequences from bleached or diseased corals *Siderastrea stellate* (Accession numbers JF835725, JF835713 and JF835652), *Favia* sp. (GQ455335) and *Porites lutea* (KC527463), respectively (Fig. 3f; Table S2d). Besides, *Endozoicomonas* OTU25 (1.1%) was highly similar to a sequence from thermally stressed sponge *Ianthella basta* (JN388027) (Fig. 3f; Table S2d). These suggested that ocean warming caused the loss of natively dominant bacteria and recruited potentially opportunistic and pathogenic members.

The combined group AW also exhibited a significantly changed microbial community when compared with group C (PERMANOVA, $F = 3.57$, $P = 0.004$) (Fig. 2i). Unclassified *Gammaproteobacteria* (1.6%) decreased significantly, whereas *Rhodobacteraceae* (13.7%) increased significantly (Fig. 2b and c; Table S2b). Thirteen differentially abundant OTUs were identified in group AW, with 3 decreased and 10 increased (Fig. 3b and c, Table S2e). The 3 decreased OTUs were consistent with those found in group W, especially the native *Gammaproteobacteria* OTU16 (0.1%) (Fig. 3f). The increased OTUs mainly belonged to members of *Rhodobacteraceae* and *Endozoicomonas*, including *Nautella* OTU7 (6%) and OTU8 (0.8%), *Roseovarius* OTU9 (0.6%), *Aliiroseovarius* OTU11 (1.2%) and *Endozoicomonas* OTU25 (2.7%) which were shared with group W (Fig. 3f; Table S2e). These indicated that the combination of ocean acidification and warming also caused the loss of natively dominant bacteria and induced potentially opportunistic members, but the change range was smaller than that in group W.

After these stressors were removed, the recovery potential of the microbial community profiles was evaluated. The composition of the active microbial community in group PA was similar to that in groups A and C, as well as T0 (Fig. 2). No significant microbial community shift (PERMANOVA, $F = 0.91$, $P = 0.5$) (Fig. 2i) or differentially abundant OTUs were observed in group PA compared with group A (Fig. 3d and e). This supported the result above that acidification had no significant effect on the sponge microbiome.

The active microbial community structure in group PW was further altered in comparison with group W (PERMANOVA, $F = 2.44$, $P = 0.02$) (Fig. 2i) and the Shannon index ($H' = 4.9 \pm 0.03$ se.) remained high (Fig. 2h). Unclassified *Alphaproteobacteria* continued to decrease (8.1%), while *Rhodobacteraceae* (38.6%), *Oceanospirillaceae* (7%), *Desulfobacteraceae* (9.6%) and *Desulfovibrionaceae* (2.4%) consistently increased (Fig. 2b to d; Table S2b). Twenty four differentially abundant OTUs were identified in group PW, with 8 decreased and 16 increased (Fig. 3d and e; Table S2f). The native *Alphaproteobacteria* OTU1 (7.9%) further decreased, and the native *Gammaproteobacteria* OTU16 became rare (0.003%) (Fig. 3f; Table S2c). Other decreased OTUs, such as

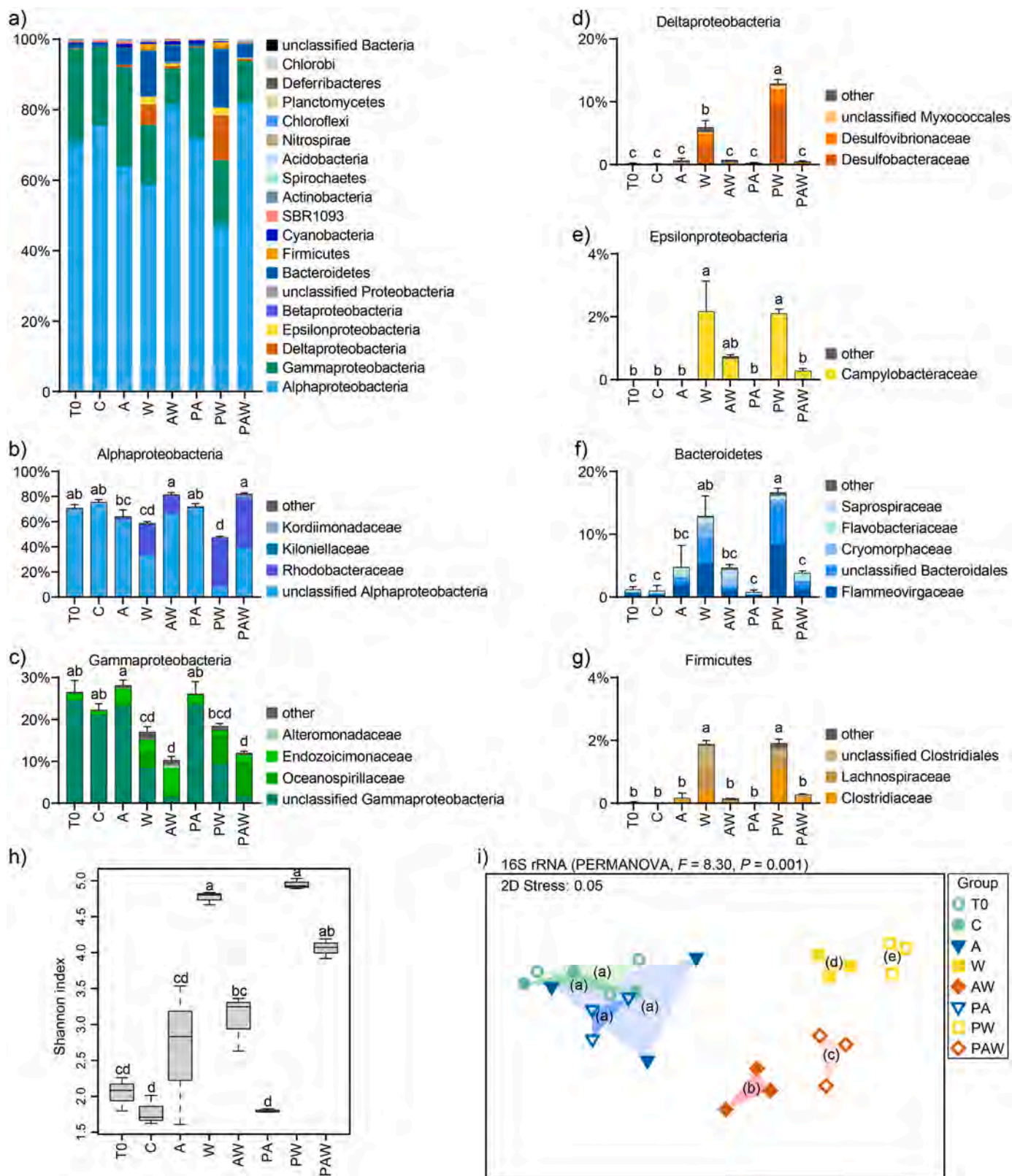


Fig. 2. Structural comparison of the active microbial community. Relative abundance of microbial phyla and proteobacterial classes (a), families within *Alphaproteobacteria* (b), *Gammaaproteobacteria* (c), *Deltaproteobacteria* (d), *Epsilonproteobacteria* (e), *Bacteroidetes* (f) and *Firmicutes* (g). Data are shown as mean \pm s.e. Bacterial families with relative abundance $< 0.05\%$ are shown as 'other'. (h) Boxplot of Shannon index. Statistical significance (ANOVA followed by Tukey's multiple comparison tests, $P < 0.05$) is illustrated with letters a, b, c and d. (i) Non-metric multidimensional scaling (NMDS) plot based on 16S rRNA assignment. F and P -values are based on PERMANOVA tests. Statistical significance ($P < 0.05$) for pairwise PERMANOVA comparisons is illustrated with letters a, b, c, d and e. T0, initial group before stress exposure; C, control; A, acidification; W, warming; AW, acidification and warming; P, stress removal group.

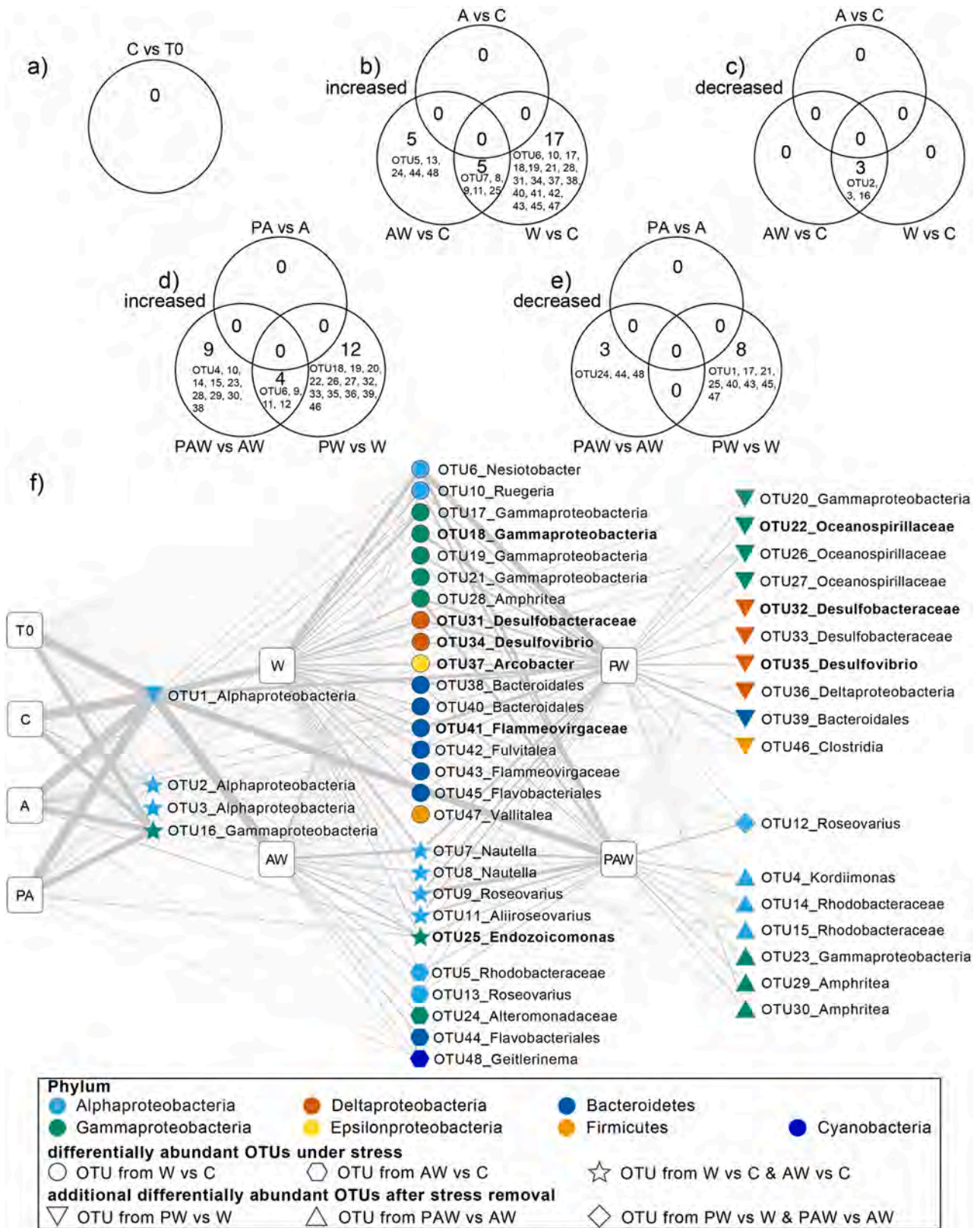


Fig. 3. Differentially abundant OTUs of the active microbial community. Number of differentially abundant OTUs in group C vs T0 (a), under stress (b and c), and after stress (d and e). (f) Relations between differentially abundant OTUs and each group. Margins of different polygons mean OTUs selected by which kind of pairwise comparison. Colors of nodes with OTU numbers represent different phyla and proteobacterial classes. Edge intensity indicates the mean relative abundance (square-root transformed) of the OTUs in each group. OTUs that matched most closely to disease, bleaching or stress associated sequences are shown in bold font. T0, initial group before stress exposure; C, control; A, acidification; W, warming; AW, acidification and warming; P, stress removal group.

Table 1

The effects of warming or/and acidification on the microbial community structure and function^a.

| Source | Degree of freedom | Mean square | F-score | P-value |
|--|-------------------|-------------|---------|---------------|
| (a) Alpha diversity - Observed OTUs | | | | |
| pH | 1 | 31389.05 | 2.284 | 0.1692 |
| Temperature | 1 | 25306.21 | 1.841 | 0.2118 |
| Temperature×pH | 1 | 1302.08 | 0.095 | 0.7661 |
| Residual | 8 | 13743.09 | | |
| (b) Alpha diversity - Shannon <i>H'</i> | | | | |
| pH | 1 | 0.49 | 1.703 | 0.2282 |
| Temperature | 1 | 8.70 | 30.123 | 0.0006 |
| Temperature×pH | 1 | 4.94 | 17.091 | 0.0033 |
| Residual | 8 | 0.29 | | |
| (c) Beta diversity - microbial community structure | | | | |
| pH | 1 | 1933.4 | 2.8035 | 0.0542 |
| Temperature | 1 | 8606.3 | 12.479 | 0.0001 |
| Temperature×pH | 1 | 2197.1 | 3.1859 | 0.0347 |
| Residual | 8 | 689.63 | | |
| (d) Microbial community function | | | | |
| pH | 1 | 162.14 | 2.77 | 0.05 |
| Temperature | 1 | 642.88 | 10.983 | 0.001 |
| Temperature×pH | 1 | 258.26 | 4.4122 | 0.003 |
| Residual | 8 | 58.534 | | |

Note:

^a Temperature and pH are taken as factors in two-way ANOVA for observed OTUs (a) and Shannon index (b); two-way PERMANOVA for microbial community structure (c) and function (d). Statistically significant effects are highlighted in bold ($P < 0.05$).

Gammaproteobacteria OTU17 (0.3%), *Flavobacteriales* OTU45 (0.2%) and *Endozoicomonas* OTU25 (0.2%), displayed a downward trajectory after small increases in group W (Fig. 3f; Table S2f). However, *Nesiotobacter* OTU6 (24.7%) continually increased and became the most abundant member in group PW, as well as bleaching-related *Gammaproteobacteria* OTU18 (4.9%). Newly increased *Oceanospirillaceae* OTU22 (0.8%), *Desulfobacteraceae* OTU32 (0.6%) and *Desulfovibrio* OTU35 (0.9%) were closely matched to sequences from diseased coral *P. lutea* (KC527511), bleached *S. stellata* (JF835713) and diseased *Favia* sp. (GQ455335), respectively (Fig. 3f; Table S2f), suggesting that more potentially opportunistic or pathogenic bacteria were stimulated after warming stress was removed.

The active microbial community structure in group PAW also further changed in comparison with group AW (PERMANOVA, $F = 2.57$, $P = 0.01$) (Fig. 2i) and the Shannon index ($H' = 4.1 \pm 0.06$ se) was still high (Fig. 2h). *Rhodobacteraceae* remained increased (39.5%) after increasing in group AW (Fig. 2b; Table S2b). Unclassified *Alphaproteobacteria* (39.2%) started dropping, while *Oceanospirillaceae* (8%) began rising (Fig. 2b and c; Table S2b). Sixteen differentially abundant OTUs were detected in group PAW, with 3 decreased and 13 increased (Fig. 3d and e; Table S2g). *Alteromonadaceae* OTU24 (0.01%), *Flavobacteriales* OTU44 (0.03%) and *Geitlerinema* OTU48 (0.03%) returned to the control level after slight increases in group AW (Fig. 3f; Table S2g). The increased OTUs were mainly affiliated with members of *Rhodobacteraceae* and *Oceanospirillaceae*, including constantly increased *Roseovarius* OTU9 (11.5%) and *Aliiroseovarius* OTU11 (3%), and newly increased *Nesiotobacter* OTU6 (8.4%), *Ruegeria* OTU10 (4%), *Roseovarius* OTU12 (2.6%), and *Amphritea* OTU28 (5%) and OTU29 (1.4%) (Fig. 3f; Table S2g). Besides, the native *Alphaproteobacteria* OTU1 (38.3%) decreased without significance (P -adjust = 0.7), and the native *Gammaproteobacteria* OTU16 became rare (0.03%) (Fig. 3f; Table S2c). These suggested that the microbial community structure did not recover after combined stress was removed.

4.2. RNA-level active microbial function change of sponge *S. vesparium* under and after warming or/and acidification

Approximately 1.06 billion merged reads from 24

metatranscriptomes (T0, C, A, W, AW, PA, PW and PAW, $n = 3$, respectively) were submitted to the MG-RAST server, with average 44.3 ± 1.5 se. million reads per sample (Table S3a). After quality control, an average of 15.7 ± 1.1 se. million reads with predicted feature were remained per sample, and about 30% of these reads were annotated as known protein. Bacterial transcriptional features were functionally annotated based on the SEED subsystems with an average of $183,408 \pm 13,674$ se and the COG database with an average of $177,834 \pm 12,922$ se. Acidification had a slight effect on the microbial functional profile, while the effects of warming and combined stress were significant (Table 1). Particularly, groups W (PERMANOVA, $F = 2.86$, $P = 0.01$) and AW ($F = 2.48$, $P = 0.02$) exhibited significant changes at subsystems function level when compared with the control (Fig. 4a).

The functional profile of group W included 434 DEGs, with 266 upregulated and 168 downregulated (Fig. 4b; Table S3b). The shifted microbiome responded to thermal stress via upregulation of genes involved in ATP synthase (e.g. alpha, gamma, delta and epsilon chains), protein chaperones (*groEL*, *groES*, *dnaK*, *hspG* and *grpE*), transcription initiation factors (*rpoD* and *rpoH*), translation elongation factors (*fusA*, *tsf* and *tuf*), oxidoreductases (superoxide dismutase and reductase, peroxidases and alkylhydroperoxidases) and flagellar motility (flagellin *fljC* and sensor kinase *cheA*) (Figs. 4c and 5a). Pathogenicity or virulence genes involved in type VI secretion system, Chv regulatory system (sensor kinase *chvG*), widespread colonization island (Tad secretion system *tadA*, *tadD*, *tadZ*, *rcpA* and pillin *flp*), autoinducer synthesis (*luxI*) and osmoregulated periplasmic glucans biosynthesis (*opgGH*) were also upregulated. However, DNA repair and defense genes encoding exonucleases, DNA helicases, CRISPRs, type I restriction-modification enzymes were downregulated (Fig. 5b). Moreover, nutrient exchange and molecular interactions were disrupted via downregulation of genes involved in ammonia assimilation (nitrogen regulatory protein P-II), creatine and creatinine degradation, coenzyme B12 and essential amino acids (methionine and tryptophan) biosynthesis, di/tricarboxylate transporter, and ABC transporter for organic ions (spermidine/putrescine and glycine betaine/proline), monosaccharides (xylose, rhamnose, inositol, ribose and glycerol-3-phosphate), oligosaccharides (alpha-glucoside and maltose/maltodextrin), branched-chain amino acid and peptides (Fig. 5b), as well as tetratricopeptide repeat (TPR) proteins (COG0457 and COG0790) (Fig. 5c). Besides, dissimilatory nitrate reduction and denitrification related periplasmic nitrate reductase (*napAB*), cytochrome cd1 nitrite reductase (*nirS*), nitric-oxide reductase (*norBC*) and nitrous-oxide reductase (*nosZ*), as well as dissimilatory sulfate reduction related sulfate adenylyltransferase (*sat*), adenylylsulfate reductase (*aprAB*) and sulfite reductase (*dsrABC*) were upregulated (Fig. 6). In group W, average 45% of *napB*, *norB*, *norC* and *nosZ* belonged to *Rhodobacteraceae* (Fig. S3), and average 82% of dissimilatory sulfate reduction DEGs belonged to deltaproteobacterial families *Desulfovibrionaceae* and *Desulfobacteraceae* (Fig. S4). The enhanced anaerobic metabolism indicated the formation of an anoxic and sulfidic microenvironment that could promote sponge tissue necrosis.

The functional profile of group AW included 326 DEGs, with 181 upregulated and 145 downregulated (Fig. 4b; Table S3c). The variation extent of functional categories in group AW was less than that in group W, since transcription initiation factors, thioredoxin-disulfide reductase, denitrification, anaerobic respiratory reductases and xylose utilization were not significantly changed in the former (Fig. 4c). Moreover, group AW had fewer DEGs than group W. In group AW, for example, genes encoding transcription factors RpoD and RpoH, cytochrome c551 peroxidase, alkylhydroperoxidase D/F, thiol peroxidase and auto-inducer synthase LuxI were not significantly upregulated (Fig. 5a), and genes encoding creatinase and D-xylose transporter XylG were not significantly downregulated (Fig. 5b). Conversely, the ethylmalonyl-CoA pathway for CO₂ assimilation was stimulated (Fig. 4c), and genes including crotonyl-CoA carboxylase/reductase (*ccr*), ethylmalonyl-CoA mutase (*ecm*), methylsuccinyl-CoA dehydrogenase (*mcd*), mesaconyl-CoA hydratase (*mch*) and L-malyl-CoA/beta-methylmalyl-CoA lyase

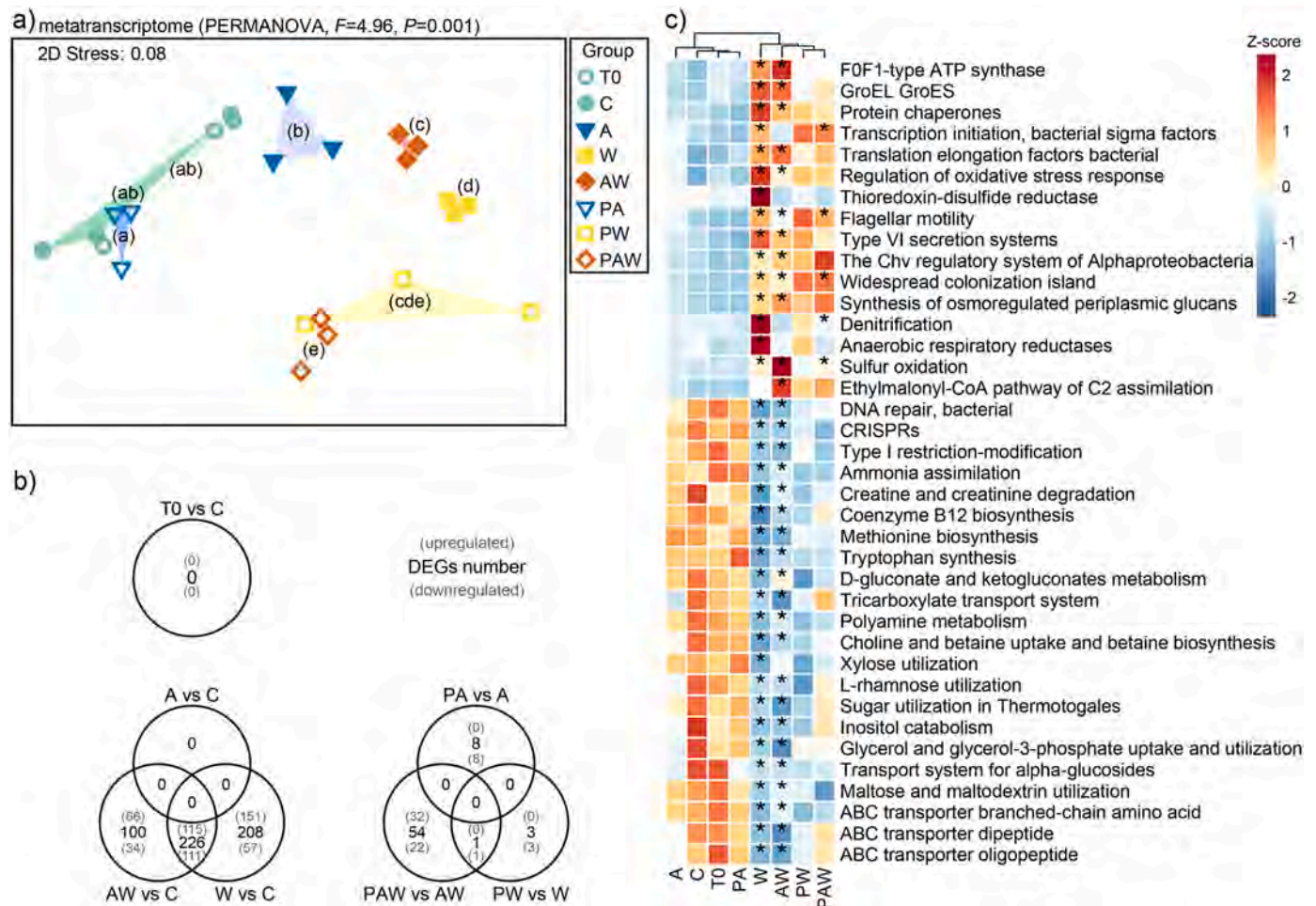


Fig. 4. Functional profile of the active microbial community. (a) Non-metric multidimensional scaling (NMDS) plot based on subsystems function level annotation. F and P -values are based on PERMANOVA tests. Statistical significance ($P < 0.05$) for pairwise PERMANOVA comparisons is illustrated with letters a, b, c, d and e. (b) Number of differentially expressed genes in group C vs T0, under and after stress. (c) Heatmap of significantly changed function categories based on subsystems level 3. Categories with FDR-adjusted ANOVA $P < 0.05$ (stress exposure group versus the control; stress removal group versus corresponding stress exposure group) are labeled with asterisks. T0, initial group before stress exposure; C, control; A, acidification; W, warming; AW, acidification and warming; P, stress removal group.

(*mclI*) were upregulated (Fig. 6). Meanwhile, group AW presented higher \log_2 fold changes in DEGs for the sulfur-oxidizing multienzyme system (*soxAXYZBCD*) than group W (4.2–6.8 vs 2.5–4.5), and enriched adenylylsulfate kinase (*cysC*) for assimilatory sulfate reduction (Fig. 6). Average 94% of these upregulated metabolic DEGs in group AW belonged to *Rhodobacteraceae* (Figs. S4 and S5). These results suggested possible interactive effects of acidification and warming stress.

The microbial functional profile of group PA differed significantly from that of group A with 8 downregulated DEGs (PERMANOVA, $F = 2.53$, $P = 0.01$), but was comparable to that of the control (PERMANOVA, $F = 0.8$, $P = 0.6$) (Fig. 4; Table S3d), indicating that the microbial function was recovered to some extent after acidification stress was removed. These DEGs, including elongation factor G-related protein (*fusA*) and type VI secretion system protein (*impC*), declined to control levels after slight increases in group A (Fig. 5a). Group PW was similar with group W (PERMANOVA, $F = 1.44$, $P = 0.15$) and did not recover to the control (PERMANOVA, $F = 2.12$, $P = 0.03$), although four genes encoding chaperones GroEL/GroES and alkylhydroperoxidases C/D was downregulated (Fig. 4; Table S3e). Group PAW was significantly different from group AW (PERMANOVA, $F = 2.65$, $P = 0.01$) with 55 DEGs (PERMANOVA, $F = 2.53$, $P = 0.01$), and did not recover to the control (PERMANOVA, $F = 2.25$, $P = 0.02$) (Fig. 4; Table S3f). Genes involved in transcription initiation (*rpoH*), flagellar motility (*fliC* and *flaA*), widespread colonization island (*pilin flp*), autoinducer synthesis

(*luxI*) and denitrification (*napA*, *nirS* and *nosZ*) were upregulated, and genes encoding ATP synthase, chaperone GroES and the Sox system were downregulated (Figs. 5a and 6). This indicated that the effects of warming and combined stress on the sponge microbiome was persistent.

5. Discussion

5.1. Warming shows greater negative effects on the *S. vesparium* microbiome than acidification

In this study, the metatranscriptome analysis indicates that single warming exhibits the most negative effects on the *S. vesparium* microbial community structure and function. On the contrary, under single acidification, the active microbial assemblage and functional profile of *S. vesparium* maintained steady, suggesting that the *S. vesparium* microbiome was tolerant to ocean acidification.

Previous research has shown that *S. vesparium* is dominated by an unclassified *Alphaproteobacteria* OTU (almost 90% relative abundance) at the DNA level (Sacristán-Soriano et al., 2020). Metatranscriptomics can gain information about active community members (Simister et al., 2012). In this study, the active microbial community of *S. vesparium* in the control was mainly composed of unclassified *Alphaproteobacteria* OTU1 (70.2%) and *Gammaproteobacteria* OTU16 (20.3%). This variation may reflect different levels of transcriptional activity of bacteria within

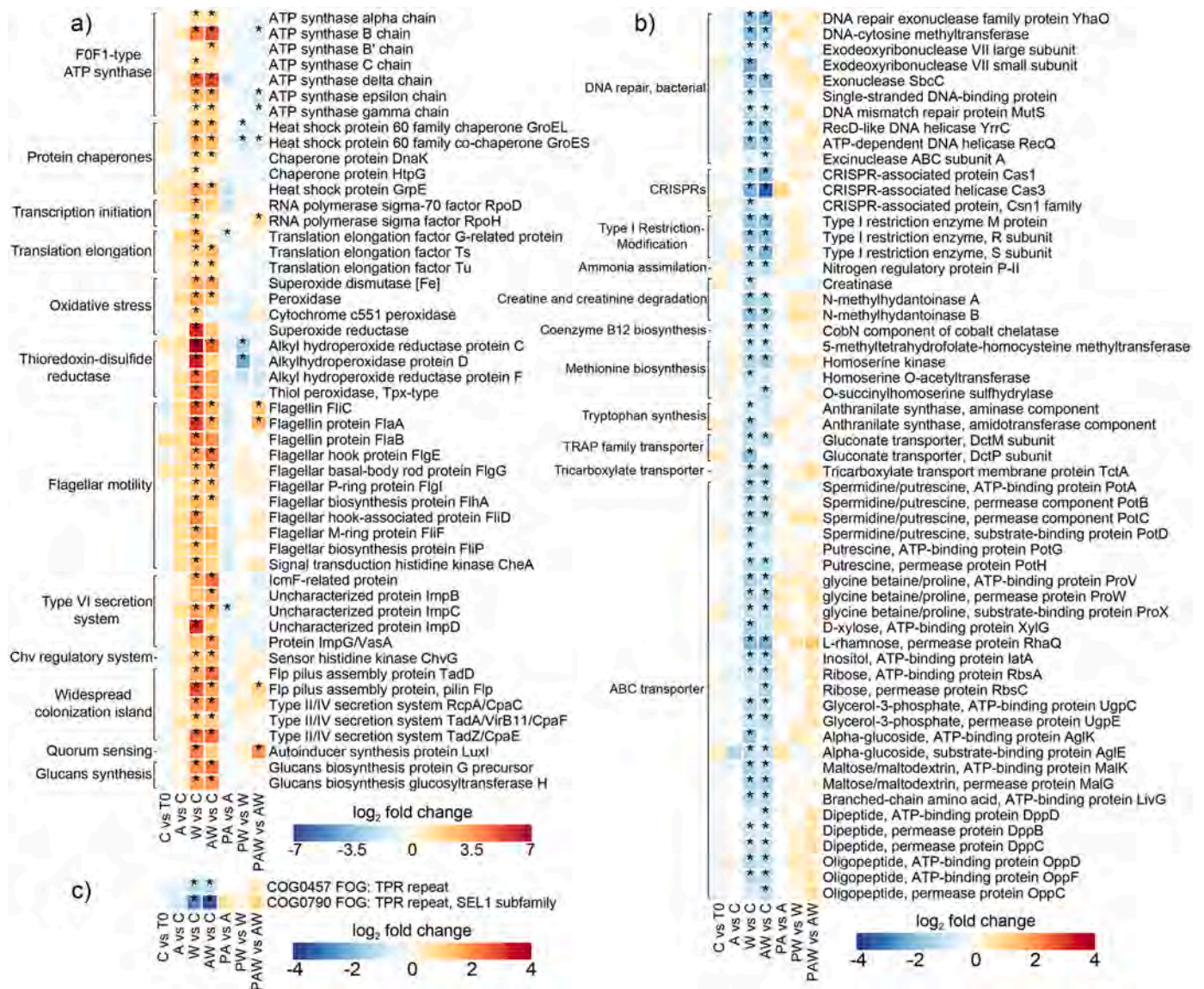


Fig. 5. Differentially expressed genes (DEGs) under stress and their change trends after stress removal. DEGs involved in stress and virulence (a), DNA repair and defense and nutrient exchange (b) are based on the SEED subsystems. DEGs encoding tetratricopeptide repeat proteins (c) are based on the COG database. DEGs are labeled with asterisks in each pairwise comparison. Colored squares represent \log_2 fold change values. T0, initial group before stress exposure; C, control; A, acidification; W, warming; AW, acidification and warming; P, stress removal group.

S. vesparium. Ocean warming significantly increased the microbial diversity in *S. vesparium*. The loss of natively dominant *Alphaproteobacteria* OTU1 and *Gammaproteobacteria* OTU16, and the rise of opportunistic microbes in *S. vesparium* under warming was similar to previous reports on sponges (Fan et al., 2013; Ramsby et al., 2018) and corals (Jessica et al., 2015). The most abundant *Rhodobacteraceae* member *Nesiotobacter* OTU6 in the warming group was closely matched to *Nesiotobacter exalbeszens* (Accession number LK054394) with unique degradation capabilities of complex aromatic compounds and advanced mechanisms for chemotaxis and cell motility (Kumar et al., 2019), allowing it to benefit from sponge tissue necrosis and proliferate rapidly in response to nutrient availability. *Bacteroidetes*, *Firmicutes* and *Oceanospirillaceae* are capable of degrading hydrocarbons (Beazley et al., 2012; Dubinsky et al., 2013) and utilizing necrotic tissues. *Desulfobacteraceae* and *Desulfovibrio* could degrade organic tissue and probably produce sulfide contributing greatly to necrosis (Arotsker et al., 2016; Sato et al., 2017). *Arcobacter* spp. (family *Campylobacteraceae*) could be opportunistic pathogens in necrotic sponges (Fan et al., 2013), diseased corals (Sato et al., 2017; Sunagawa et al., 2009) and moribund oysters (Lokmer and

Wegner, 2015). *Endozoicomonas* spp. found in thermally stressed and necrotic sponges (Fan et al., 2013; Luter et al., 2012) could be opportunistic genotypes (Neave et al., 2017). In group W, significantly increased *Gammaproteobacteria* OTU18, *Desulfobacteraceae* OTU31, *Desulfovibrio* OTU34, *Arcobacter* OTU37, *Flammeovirgaceae* OTU41 and *Endozoicomonas* OTU25 matched most closely to organisms in bleached or diseased corals and thermally stressed sponges. These indicated that warming disrupted the microbiome stability and triggered potentially opportunistic and pathogenic bacteria in *S. vesparium*.

Rhodobacteraceae could be indicators of *S. vesparium* under future ocean circumstances since this family became predominant under single warming and combined warming and acidification stress. *Rhodobacteraceae* can interact with aquatic micro- and macroorganisms in mutualistic and pathogenic ways (Luo and Moran, 2014). Members of this family have been reported as opportunistic colonizers in diseased sponges (Belikov et al., 2019; Deignan et al., 2018; Kulakova et al., 2018) and corals (MacKnight et al., 2021; Welsh et al., 2017). *Rhodobacteraceae* are also suggested to be indicators of stressed reefs (Glasl et al., 2019) and corals (Pootakham et al., 2019). A previous study has

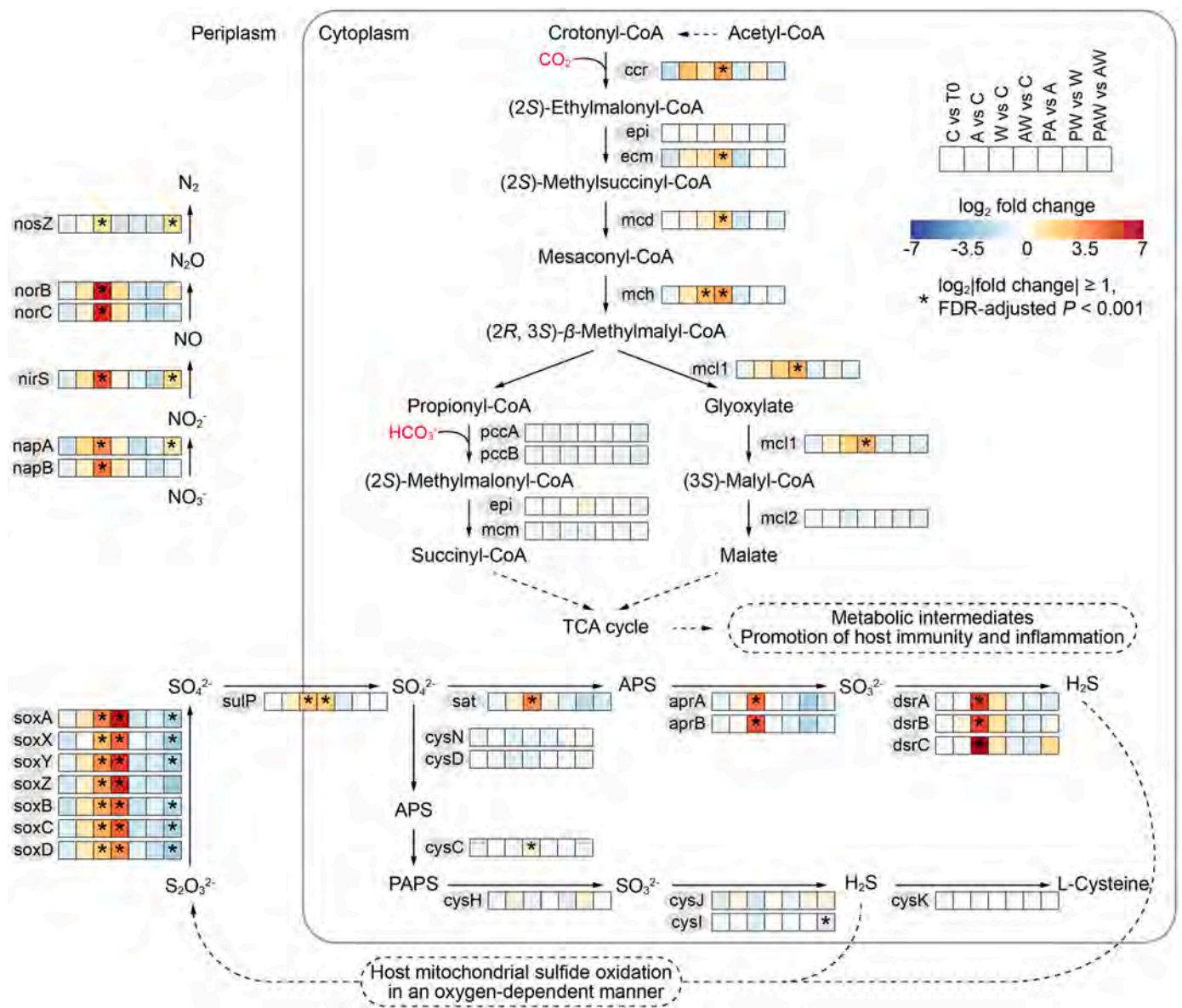


Fig. 6. Microbial metabolic pathways related to carbon, nitrogen and sulfur metabolisms. Inorganic carbon is highlighted in red. Differentially expressed genes (DEGs) are labeled with asterisks in each pairwise comparison. Colored squares represent \log_2 fold change values. TO, initial group before stress exposure; C, control; A, acidification; W, warming; AW, acidification and warming; P, stress removal group.

confirmed one *Rhodobacteraceae*-affiliated bacterium and one *Rhizoglyphus*-affiliated fungus as aetiological agents of sponge necrosis syndrome in *Callyspongia (Euplacella) aff. biru* (Sweet et al., 2015). Besides, several studies have shown that marine *Rhodobacteraceae* are closely associated with sponges (Knobloch et al., 2019; Morrow et al., 2016; Podell et al., 2020; Webster et al., 2011) and may facilitate the sponge holobionts to cope with pollutants (Turon et al., 2019). In this study, all significantly increased *Rhodobacteraceae*-affiliated OTUs were closely matched to sequences retrieved from water, sediments and corals, and were rare in the control (each less than 0.1%), suggesting that they were possible opportunists when the microbial assemblage broke down.

Ocean warming seriously disrupted the functional homeostasis in the *S. vesparium* microbiome and had the most influence on the microbial community function. Microbial symbionts can regulate the assimilation of ammonium secreted by sponge host via nitrogen regulatory protein PII (Thomas et al., 2010). Here the decreased expression of this gene could cause nitrogen cycle imbalance, probably resulting in toxic ammonium accumulation and eventually declining host health.

Additionally, microbial symbionts can conduct nutrient exchange with sponge host by transporters, degrade creatine and creatinine produced by the host as sources of carbon and nitrogen, and synthesize essential B-vitamins and amino acids to satisfy the host's demand (Fan et al., 2012). Microbial symbionts can use eukaryotic-like proteins containing TPRs to escape host phagocytosis, and require DNA recombination and repair enzymes, CRISPRs, and restriction-modification systems to manipulate genetic rearrangement and exchange in the symbiont community (Fan et al., 2012). In this study, the expression of genes related to symbiosis was significantly depressed under warming, indicating that native symbionts and their associated functions were reduced. Instead, the shifted microbiome could grow rapidly and deal with thermal or host oxidative stress via upregulated genes encoding ATP synthase, transcription and translation factors, protein chaperones and antioxidant enzymes. The enriched flagellar motility facilitated the transposition of motile colonizers towards nutrient source from necrotic tissues. Altogether, these results suggested that ocean warming disrupted the nutrient exchange and molecular interactions in *S. vesparium* holobiont,

consistent with previous observations in thermally stressed *R. odorabile* (Fan et al., 2013) and *S. flabelliformis* (Botté et al., 2023).

Ocean warming also stimulated virulence activity and anaerobic metabolism in the *S. vesparium* microbiome to promote sponge tissue necrosis. The Chv regulatory system can activate the type VI secretion system (Wu et al., 2012), and the latter can directly deliver toxic effectors to eukaryotic cells and target other bacteria in polymicrobial infections (Ho et al., 2014). The Tad secretion system is essential for biofilm formation, colonization and pathogenesis (Tomich et al., 2007), and osmoregulated periplasmic glucans are implicated in bacterial pathogenicity (Bontemps-Gallo et al., 2017). Acyl-homoserine lactones produced by autoinducer synthase LuxI can mediate quorum sensing and control bacterial population behaviors and gene expression, including biofilm formation and virulence factor production (Hense and Schuster, 2015). The enrichment of these genes involved in virulence under warming stress could facilitate potentially opportunistic and pathogenic bacteria to adhere and invade host cells, finally disrupting the holobiont health. Besides, dissimilatory nitrate reduction and denitrification mainly undertaken by *Rhodobacteraceae*, and dissimilatory sulfate reduction primarily undertaken by *Desulfovibrionaceae* and *Desulfobacteraceae* were enriched under warming, indicating that an anoxic and sulfidic microenvironment was formed (Plugge et al., 2011; Strohm et al., 2007), and undoubtedly intensifying the sponge holobiont's collapse and tissue necrosis.

A previous study has found that the bioeroding sponge *C. orientalis* cannot regain *Symbiodinium* or restore its baseline microbial community, and gain more opportunistic filamentous *Cyanobacteria* after thermal-induced bleaching (Ramsby et al., 2018). In this study, we evaluated the *S. vesparium* microbiome's recovery potential. The *S. vesparium* microbiome maintained stable during and after acidification treatment. Slight disturbances in several genes (e.g. *fusA* and *impC*) caused by acidification were eliminated once the acidity returned to normal. After warming stress, more potentially opportunistic and pathogenic members of *Nesiotobacter*, *Oceanospirillaceae*, *Desulfobacteraceae*, *Desulfovibrionaceae*, *Bacteroidetes* and *Firmicutes* outcompeted the native *Alphaproteobacteria* OTU1 and *Gammaproteobacteria* OTU16. Accordingly, warming could induce irreversible destabilization in the microbial structure and function of sponge *S. vesparium*, although sponges are generally thought to be more resistant to environmental change than several currently dominant benthic organisms, such as corals (Bell et al., 2018; Schönberg et al., 2017).

5.2. The interactive effects between ocean acidification and warming on the *S. vesparium* microbiome

In this study, the combined stress of ocean warming and acidification exhibited a significant effect on the microbial community structure of *S. vesparium*, but the degree of microbial dysbiosis was less than that caused by single warming. The community shift mainly included a dramatic decrease in native *Gammaproteobacteria* OTU16 and a significant increase in *Rhodobacteraceae*, whereas potentially opportunistic and pathogenic members of *Nesiotobacter*, *Oceanospirillaceae*, *Desulfobacteraceae*, *Desulfovibrionaceae*, *Campylobacteraceae*, *Bacteroidetes*, and *Firmicutes* were not significantly increased. Similarly, the destabilization of microbial function caused by warming was lessened by simultaneous acidification, as some related functions were not enhanced under combined stress. For instance, genes encoding sigma factors RpoD and RpoH, which can regulate a variety of genes involving growth and stress response (Ishihama, 2000), cytochrome c551 peroxidase, which is synthesized under anaerobic conditions and uses H₂O₂ as a terminal oxidant to promote respiration (Imlay, 2019), and autoinducer synthase LuxI, which can mediate quorum sensing to control biofilm formation and virulence (Hense and Schuster, 2015), were not significantly upregulated under combined stress. Besides, denitrification and dissimilatory reduction of nitrate and sulfate under anoxic conditions were also not significantly enriched. These demonstrated that acidification could

partially mitigate the negative effects of warming on the microbial community structure and function.

The interactive effects of ocean warming and acidification on sponges have been reported from the aspect of physiological responses, with acidification exacerbating warming stress in heterotrophic species but reducing warming stress in phototrophic species (Bennett et al., 2017). When more inorganic carbon is available, the increased productivity of photosymbionts is speculated to enable phototrophic sponges *Carteriospongia foliascens* and *Cymbastela coralliophila* to lessen the impact of warming stress. Moreover, the enrichment of photoheterotrophic *Rhodobacteraceae* and the stable population of other photosymbionts in sponge *Neopetrosia compacta* have been inferred to ameliorate the effects of acidification and warming (Posadas et al., 2022). However, the detailed molecular mechanisms of these interactive effects are not yet clear. In this study, *S. vesparium* is a heterotrophic type because it is an azooxanthellate sponge and harbors very few cyanobacteria (Sacristán-Soriano et al., 2020). The ethylmalonyl-CoA pathway primarily undertaken by increased *Rhodobacteraceae*, was enhanced under combined stress (Fig. 6). Photoheterotrophic *Rhodobacteraceae* can assimilate CO₂ via the ethylmalonyl-CoA pathway, which generates succinyl-CoA and malate and channels them into the tricarboxylic acid (TCA) cycle to support biomass production (Bill et al., 2017). These bacteria could be phagocytosed by the sponge host and then translocated these metabolic intermediates to host cells for energy supply and macromolecular synthesis. Moreover, some metabolic intermediates of the TCA cycle are emerging as important signals in immunity and inflammation. For example, the accumulated succinate in immune cells can stabilize the transcription factor hypoxia-inducible factor-1 α (HIF-1 α), which then enhances the expression of HIF-1 α -dependent genes, such as cytokine interleukin1 β (IL-1 β), to promote immunity and inflammation (Mills and O'Neill, 2014). Likewise, exogenous malate potentiates zebrafish survival against *Vibrio alginolyticus* infection by boosting the innate immune response and promoting the generation of reactive oxygen species and nitrogen oxide (Yang et al., 2020). Therefore, the enriched ethylmalonyl-CoA pathway under combined warming and acidification may not only benefit the increased *Rhodobacteraceae*, but also possibly provide *S. vesparium* with additional metabolic intermediates and promote its immunity and inflammation to reduce the invasion of potentially opportunistic and pathogenic bacteria and to alleviate the negative effects of warming.

Furthermore, in this study, the enhanced Sox system was predominantly undertaken by *Rhodobacteraceae* to completely oxidize thiosulfate to sulfate, and the expression levels of *sox* genes were higher under combined stress than under single warming (Fig. 6). Thiosulfate has been evaluated as a biomarker of mammalian colon inflammation, which is associated with the generation of toxic hydrogen sulfide (Daeffler et al., 2017). It can be formed in mammalian and invertebrate mitochondria through an oxygen-dependent sulfide oxidation pathway for detoxification (Hildebrandt and Grieshaber, 2008), and stimulates the expression of *sox* genes in *Rhodobacteraceae* to gain additional energy for cellular metabolism and growth (Muthusamy et al., 2014). Therefore, the higher expression levels of *sox* genes under combined stress than under single warming not only reflected higher thiosulfate production by *S. vesparium* to supply *Rhodobacteraceae* with more energy for growth, probably benefiting the host, but also indicated more oxygen availability for the sponge to support sulfide detoxification and aerobic energy metabolism. Moreover, ocean warming can reduce sponge pumping activity (Massaro et al., 2012; Stevenson et al., 2020). The low pumping activity decreases oxygen concentrations inside the sponge mesohyl and even causes anoxic conditions to favor anaerobic symbionts and anaerobic metabolism (Hoffmann et al., 2008; Schläppy et al., 2010), e.g. the enhanced denitrification and dissimilatory reduction of nitrate and sulfate under single warming in the present study were indicated. It is worth noting that the interaction of acidification and warming has been reported to dampen the negative effects of warming on the pumping activity of sponge *Aphrocallistes vastus* to a certain range

(Stevenson et al., 2020).

6. Conclusions

This study demonstrates the response of the active microbiota of the bioeroding sponge *S. vesparium* under ocean warming or/and acidification (32 °C or/and pH 7.7) in a laboratory simulation system using metatranscriptomics. While tolerant to acidification, the *S. vesparium* microbiome is disrupted by warming or simultaneous warming and acidification. Warming has the most negative impact on the microbiome, including the dramatic decrease of native microbial symbionts and the induction of potentially opportunistic and pathogenic bacteria with enhanced virulence functions and anaerobic metabolism. Importantly, interactive effects of ocean acidification and warming on the structure and function of the bioeroding sponge *S. vesparium* microbiome are suggested. The microbiome fails to recover after warming or combined stress is removed. This study suggests that warming or combined warming and acidification may irreversibly destabilize the *S. vesparium* microbial community structure and function, and provides a mechanistic understanding of the interactive effects of acidification and warming on the sponge microbiome. Further studies performing metabolic and physiological investigations under these conditions are required to better understand the vulnerability of the bioeroding sponge *S. vesparium* under warming or/and acidification.

CRedit authorship contribution statement

Guangjun Chai: Conceptualization, Methodology, Software, Validation, Formal analysis, Investigation, Data curation, Writing – original draft, Writing – review & editing, Visualization. **Jinlong Li:** Conceptualization, Methodology, Investigation. **Zhiyong Li:** Conceptualization, Resources, Supervision, Funding acquisition, Writing – review & editing.

Declaration of Competing Interest

The authors declare that they have no known competing financial interests or personal relationships that could have appeared to influence the work reported in this paper.

Data Availability

Data will be made available on request.

Acknowledgements

This work was supported by the National Natural Science Foundation of China (Grant No. 31861143020, 41776138, U1301131). We appreciate Xuwen National Coral Reef Nature Reserve to provide the condition of simulation experiment. We acknowledge the Center for High Performance Computing at Shanghai Jiao Tong University for computation support.

Appendix A. Supporting information

Supplementary data associated with this article can be found in the online version at [doi:10.1016/j.micres.2023.127542](https://doi.org/10.1016/j.micres.2023.127542).

References

Apprill, A., 2017. Marine animal microbiomes: toward understanding host-microbiome interactions in a changing ocean. *Front Mar. Sci.* 4, 222. <https://doi.org/10.3389/fmars.2017.00222>.

Arotsker, L., Kramarsky-Winter, E., Ben-Dov, E., Kushmaro, A., 2016. Microbial transcriptome profiling of black band disease in a *Faviid* coral during a seasonal disease peak. *Dis. Aquat. Org.* 118, 77–89. <https://doi.org/10.3354/dao02952>.

Beazley, M.J., Martinez, R.J., Rajan, S., et al., 2012. Microbial community analysis of a coastal salt marsh affected by the *Deepwater Horizon* oil spill. *PLoS One* 7, e41305. <https://doi.org/10.1371/journal.pone.0041305>.

Belikov, S., Belkova, N., Butina, T., et al., 2019. Diversity and shifts of the bacterial community associated with Baikal sponge mass mortalities. *PLoS One* 14, e0213926. <https://doi.org/10.1371/journal.pone.0213926>.

Bell, J.J., Bennett, H.M., Rovellini, A., Webster, N.S., 2018. Sponges to be winners under near-future climate scenarios. *Bioscience* 68, 955–968. <https://doi.org/10.1093/biosci/biy142>.

Bennett, H.M., Altenrath, C., Woods, L., et al., 2017. Interactive effects of temperature and pCO₂ on sponges: from the cradle to the grave. *Glob. Change Biol.* 23, 2031–2046. <https://doi.org/10.1111/gcb.13474>.

Bill, N., Tomasch, J., Riemer, A., et al., 2017. Fixation of CO₂ using the ethylmalonyl-CoA pathway in the photoheterotrophic marine bacterium *Dinoroseobacter shibae*. *Environ. Microbiol.* 19, 2645–2660. <https://doi.org/10.1111/1462-2920.13746>.

Bokulich, N.A., Subramanian, S., Faith, J.J., et al., 2013. Quality-filtering vastly improves diversity estimates from Illumina amplicon sequencing. *Nat. Methods* 10, 57–59. <https://doi.org/10.1038/nmeth.2276>.

Bokulich, N.A., Kaehler, B.D., Rideout, J.R., et al., 2018. Optimizing taxonomic classification of marker-gene amplicon sequences with QIIME 2's q2-feature-classifier plugin. *Microbiome* 6, 90. <https://doi.org/10.1186/s40168-018-0470-z>.

Bolger, A.M., Lohse, M., Usadel, B., 2014. Trimmomatic: a flexible trimmer for Illumina sequence data. *Bioinformatics* 30, 2114–2120. <https://doi.org/10.1093/bioinformatics/btu170>.

Bolyen, E., Rideout, J.R., Dillon, M.R., et al., 2019. Reproducible, interactive, scalable and extensible microbiome data science using QIIME 2. *Nat. Biotechnol.* 37, 852–857. <https://doi.org/10.1038/s41587-019-0209-9>.

Bontemps-Gallo, S., Bohin, J.-P., Lacroix, J.-M., Slauch, J.M., 2017. Osmoregulated periplasmic glucans. *EcoSal*. <https://doi.org/10.1128/ecosalplus.ESP-0001-2017>.

Botté, E.S., Nielsen, S., Abdul Wahab, M.A., et al., 2019. Changes in the metabolic potential of the sponge microbiome under ocean acidification. *Nat. Commun.* 10, 4134. <https://doi.org/10.1038/s41467-019-12156-y>.

Botté, E.S., Bennett, H., Engelberts, J.P., et al., 2023. Future ocean conditions induce necrosis, microbial dysbiosis and nutrient cycling imbalance in the reef sponge *Stylissa flabelliformis*. *ISME Commun.* 3, 53. <https://doi.org/10.1038/s43705-023-00247-3>.

Bourne, D.G., Morrow, K.M., Webster, N.S., 2016. Insights into the coral microbiome: underpinning the health and resilience of reef ecosystems. *Annu Rev. Microbiol.* 70, 317–340. <https://doi.org/10.1146/annurev-micro-102215-095440>.

Bray, J.R., Curtis, J.T., 1957. An ordination of the upland forest communities of southern Wisconsin. *Ecol. Monogr.* 27, 325–349. <https://doi.org/10.2307/1942268>.

Butler, M.J., Hunt, J.H., Herrnkind, W.F., et al., 1995. Cascading disturbances in Florida Bay, USA: cyanobacteria blooms, sponge mortality, and implications for juvenile spiny lobsters *Panulirus argus*. *Mar. Ecol. Prog. Ser.* 129, 119–125. <https://doi.org/10.3354/meps129119>.

Butler, M.J., Weisz, J.B., Butler, J., 2018. The effects of water quality on back-reef sponge survival and distribution in the Florida Keys, Florida (USA). *J. Exp. Mar. Biol. Ecol.* 503, 92–99. <https://doi.org/10.1016/j.jembe.2018.03.001>.

Daeffler, K.N.M., Galley, J.D., Sheth, R.U., et al., 2017. Engineering bacterial thiosulfate and tetrathionate sensors for detecting gut inflammation. *Mol. Syst. Biol.* 13, 923. <https://doi.org/10.15252/msb.20167416>.

Deignan, L.K., Pawlik, J.R., Erwin, P.M., 2018. *Agelas* wasting syndrome alters prokaryotic symbiont communities of the Caribbean brown tube sponge, *Agelas tubulata*. *Micro Ecol.* 76, 459–466. <https://doi.org/10.1007/s00248-017-1135-3>.

Doney, S.C., Ruckelshaus, M., Duffy, J.E., et al., 2012. Climate change impacts on marine ecosystems. *Annu Rev. Mar. Sci.* 4, 11–37. <https://doi.org/10.1146/annurev-marine-041911-111611>.

Dubinsky, E.A., Conrad, M.E., Chakraborty, R., et al., 2013. Succession of hydrocarbon-degrading bacteria in the aftermath of the *Deepwater Horizon* oil spill in the Gulf of Mexico. *Environ. Sci. Technol.* 47, 10860–10867. <https://doi.org/10.1021/es401676y>.

Engelberts, J.P., Robbins, S.J., de Goeij, J.M., et al., 2020. Characterization of a sponge microbiome using an integrative genome-centric approach. *ISME J.* 14, 1100–1110. <https://doi.org/10.1038/s41396-020-0591-9>.

Fan, L., Reynolds, D., Liu, M., et al., 2012. Functional equivalence and evolutionary convergence in complex communities of microbial sponge symbionts. *Proc. Natl. Acad. Sci. USA* 109, E1878–E1887. <https://doi.org/10.1073/pnas.1203287109>.

Fan, L., Liu, M., Simister, R., et al., 2013. Marine microbial symbiosis heats up: the phylogenetic and functional response of a sponge holobiont to thermal stress. *ISME J.* 7, 991–1002. <https://doi.org/10.1038/ismej.2012.165>.

Glasl, B., Bourne, D.G., Frade, P.R., et al., 2019. Microbial indicators of environmental perturbations in coral reef ecosystems. *Microbiome* 7, 94. <https://doi.org/10.1186/s40168-019-0705-7>.

He, L.M., Liu, F., Karuppiah, V., et al., 2014. Comparisons of the fungal and protistan communities among different marine sponge holobionts by pyrosequencing. *Micro Ecol.* 67, 951–961. <https://doi.org/10.1007/s00248-014-0393-6>.

Hense, B.A., Schuster, M., 2015. Core principles of bacterial autoinducer systems. *Microbiol Mol. Biol. Rev.* 79, 153–169. <https://doi.org/10.1128/MMBR.00024-14>.

Hildebrandt, T.M., Grieshaber, M.K., 2008. Three enzymatic activities catalyze the oxidation of sulfide to thiosulfate in mammalian and invertebrate mitochondria. *FEBS J.* 275, 3352–3361. <https://doi.org/10.1111/j.1742-4658.2008.06482.x>.

Ho, B.T., Dong, T.G., Mekalanos, J.J., 2014. A view to a kill: the bacterial type VI secretion system. *Cell Host Microbe* 15, 9–21. <https://doi.org/10.1016/j.chom.2013.11.008>.

Hoegh-Guldberg, O., Bruno, J.F., 2010. The impact of climate change on the world's marine ecosystems. *Science* 328, 1523–1528. <https://doi.org/10.1126/science.1189930>.

- Hoegh-Guldberg, O., Mumby, P.J., Hooten, A.J., et al., 2007. Coral reefs under rapid climate change and ocean acidification. *Science* 318, 1737–1742. <https://doi.org/10.1126/science.1152509>.
- Hoffmann, F., Roy, H., Bayer, K., et al., 2008. Oxygen dynamics and transport in the Mediterranean sponge *Aplysina aerophoba*. *Mar. Biol.* 153, 1257–1264. <https://doi.org/10.1007/s00227-008-0905-3>.
- Imlay, J.A., 2019. Where in the world do bacteria experience oxidative stress. *Environ. Microbiol.* 21, 521–530. <https://doi.org/10.1111/1462-2920.14445>.
- IPCC, 2014. Climate change 2014: synthesis report. contribution of working groups I, II and III to the fifth assessment report of the Intergovernmental Panel on Climate Change. IPCC, Geneva, Switzerland. (<https://www.ipcc.ch/report/ar5/syr/>).
- Ishihama, A., 2000. Functional Modulation of *Escherichia coli* RNA Polymerase. *Annu Rev. Microbiol.* 54, 499–518. <https://doi.org/10.1146/annurev.micro.54.1.499>.
- Jessica, T., Nachshon, S., Messer, L.F., et al., 2015. Increased seawater temperature increases the abundance and alters the structure of natural *Vibrio* populations associated with the coral *Pocillopora damicornis*. *Front Microbiol.* 6, 432. <https://doi.org/10.3389/fmicb.2015.00432>.
- Kandler, N.M., Abdul Wahab, M.A., Noonan, S.H.C., et al., 2018. In situ responses of the sponge microbiome to ocean acidification. *FEMS Microbiol Ecol.* 94, fy205. <https://doi.org/10.1093/femsec/fiy205>.
- Katoh, K., Standley, D.M., 2013. MAFFT multiple sequence alignment software version 7: improvements in performance and usability. *Mol. Biol. Evol.* 30, 772–780. <https://doi.org/10.1093/molbev/mst010>.
- Knobloch, S., Jóhannsson, R., Marteinsson, V., 2019. Bacterial diversity in the marine sponge *Halichondria panicea* from Icelandic waters and host-specificity of its dominant symbiont “*Candidatus Halichondriabacter symbioticus*”. *FEMS Microbiol Ecol.* 95, fy220. <https://doi.org/10.1093/femsec/fiy220>.
- Kulakov, N.V., Sakirko, M.V., Adeshin, R.V., et al., 2018. Brown rot syndrome and changes in the bacterial community of the Baikal spring *Lubomirskia baicalensis*. *Micro Ecol.* 75, 1024–1034. <https://doi.org/10.1007/s00248-017-1097-5>.
- Kumar, A.G., Mathew, N.C., Sujitha, K., et al., 2019. Genome analysis of deep sea piezotolerant *Nesiotobacter exalbescens* COD22 and toluene degradation studies under high pressure condition. *Sci. Rep.* 9, 18724. <https://doi.org/10.1038/s41598-019-55115-9>.
- Lesser, M.P., Fiore, C., Slattery, M., Zaneveld, J., 2016. Climate change stressors destabilize the microbiome of the Caribbean barrel sponge, *Xestospongia muta*. *J. Exp. Mar. Biol. Ecol.* 475, 11–18. <https://doi.org/10.1016/j.jembe.2015.11.004>.
- Lesser, M.P., Sabrina Pankey, M., Slattery, M., et al., 2022. Microbiome diversity and metabolic capacity determines the trophic ecology of the holobiont in Caribbean sponges. *ISME Commun.* 2, 112. <https://doi.org/10.1038/s43705-022-00196-3>.
- Letourneau, M.L., Hopkinson, B.M., Fitt, W.K., Medeiros, P.M., 2020. Molecular composition and biodegradation of loggerhead sponge *Spheciospongia vesparium* exhalant dissolved organic matter. *Mar. Environ. Res.* 162, 105130. <https://doi.org/10.1016/j.marenvres.2020.105130>.
- Li, J., Chai, G., Xiao, Y., Li, Z., 2023. The impacts of ocean acidification, warming and their interactive effects on coral prokaryotic symbionts. *Environ. Microbiol.* 18, 49. <https://doi.org/10.1186/s40793-023-00505-w>.
- Lokmer, A., Wegner, K.M., 2015. Hemolymph microbiome of Pacific oysters in response to temperature, temperature stress and infection. *ISME J.* 9, 670–682. <https://doi.org/10.1038/ismej.2014.160>.
- Love, M.I., Huber, W., Anders, S., 2014. Moderated estimation of fold change and dispersion for RNA-seq data with DESeq2. *Genome Biol.* 15, 550. <https://doi.org/10.1186/s13059-014-0550-8>.
- Luo, H.W., Moran, M.A., 2014. Evolutionary ecology of the marine *Roseobacter* clade. *Microbiol Mol. Biol. Rev.* 78, 573–587. <https://doi.org/10.1128/MMBR.00020-14>.
- Luter, H.M., Whalan, S., Webster, N.S., 2012. Thermal and sedimentation stress are unlikely causes of brown spot syndrome in the coral reef sponge, *Ianthella basta*. *PLoS One* 7, e39779. <https://doi.org/10.1371/journal.pone.0039779>.
- Luter, H.M., Andersen, M., Versteegen, E., et al., 2020. Cross-generational effects of climate change on the microbiome of a photosynthetic sponge. *Environ. Microbiol.* 22, 4732–4744. <https://doi.org/10.1111/1462-2920.15222>.
- MacKnight, N.J., Cobleigh, K., Lasseigne, D., et al., 2021. Microbial dysbiosis reflects disease resistance in diverse coral species. *Commun. Biol.* 4, 679. <https://doi.org/10.1038/s42003-021-02163-5>.
- Masella, A.P., Bartram, A.K., Truszkowski, J.M., et al., 2012. PANDAseq: paired-end assembler for illumina sequences. *BMC Bioinforma.* 13, 31. <https://doi.org/10.1186/1471-2105-13-31>.
- Massaro, A.J., Weisz, J.B., Hill, M.S., Webster, N.S., 2012. Behavioral and morphological changes caused by thermal stress in the Great Barrier Reef sponge *Rhopaloeides odorabile*. *J. Exp. Mar. Biol. Ecol.* 416–417, 55–60. <https://doi.org/10.1016/j.jembe.2012.02.008>.
- McDonald, D., Price, M.N., Goodrich, J., et al., 2012. An improved Greengenes taxonomy with explicit ranks for ecological and evolutionary analyses of bacteria and archaea. *ISME J.* 6, 610–618. <https://doi.org/10.1038/ismej.2011.139>.
- Meyer, F., Paarmann, D., D'Souza, M., et al., 2008. The metagenomics RAST server - a public resource for the automatic phylogenetic and functional analysis of metagenomes. *BMC Bioinforma.* 9, 386. <https://doi.org/10.1186/1471-2105-9-386>.
- Mills, E., O'Neill, L.A.J., 2014. Succinate: a metabolic signal in inflammation. *Trends Cell Biol.* 24, 313–320. <https://doi.org/10.1016/j.tcb.2013.11.008>.
- Morrow, K.M., Bourne, D.G., Humphrey, C., et al., 2015. Natural volcanic CO₂ seeps reveal future trajectories for host-microbial associations in corals and sponges. *ISME J.* 9, 894–908. <https://doi.org/10.1038/ismej.2014.188>.
- Morrow, K.M., Fiore, C.L., Lesser, M.P., 2016. Environmental drivers of microbial community shifts in the giant barrel sponge, *Xestospongia muta*, over a shallow to mesophotic depth gradient. *Environ. Microbiol.* 18, 2025–2038. <https://doi.org/10.1111/1462-2920.13226>.
- Muthusamy, S., Baltar, F., Gonazlez, J.M., Pinhasi, J., 2014. Dynamics of metabolic activities and gene expression in the *Roseobacter* clade bacterium *Phaeobacter* sp strain MED193 during growth with thiosulfate. *Appl. Environ. Microbiol.* 80, 6933–6942. <https://doi.org/10.1128/AEM.02038-14>.
- Neave, M.J., Michell, C.T., Apprill, A., Voolstra, C.R., 2017. *Endozoicomonas* genomes reveal functional adaptation and plasticity in bacterial strains symbiotically associated with diverse marine hosts. *Sci. Rep.* 7, 40579. <https://doi.org/10.1038/srep40579>.
- Pedregosa, F., Varoquaux, G., Gramfort, A., et al., 2011. Scikit-learn: machine learning in python. *J. Mach. Learn. Res.* 12, 2825–2830. <https://doi.org/10.48550/arXiv.1201.0490>.
- Pierrot, D.E., Wallace, D.W.R., Lewis, E., 2006. MS Excel program developed for CO₂ system calculations. ORNL Environ. Sci. Div., Oak Ridge, TN. <https://doi.org/10.3334/CDIAC/otg.CO2SYS.XLS.CDIAC105a>.
- Pita, L., Rix, L., Slaby, B.M., et al., 2018. The sponge holobiont in a changing ocean: from microbes to ecosystems. *Microbiome* 6, 46. <https://doi.org/10.1186/s40168-018-0428-1>.
- Plugge, C.M., Zhang, W.W., Scholten, J.C.M., Stams, A.J.M., 2011. Metabolic flexibility of sulfate-reducing bacteria. *Front Microbiol.* 2, 81. <https://doi.org/10.3389/fmicb.2011.00081>.
- Podell, S., Blanton, J.M., Oliver, A., et al., 2020. A genomic view of trophic and metabolic diversity in clade-specific *Lamellodysidea* sponge. *Micro Micro* 8, 97. <https://doi.org/10.1186/s40168-020-00877-y>.
- Pootakham, W., Mhuantong, W., Yoocha, T., et al., 2019. Heat-induced shift in coral microbiome reveals several members of the *Rhodobacteraceae* family as indicator species for thermal stress in *Porites lutea*. *MicrobiologyOpen* 8, e935. <https://doi.org/10.1002/mbo3.935>.
- Posadas, N., Baquiran, J.I.P., Nada, M.A.L., et al., 2022. Microbiome diversity and host immune functions influence survivorship of sponge holobionts under future ocean conditions. *ISME J.* 16, 58–67. <https://doi.org/10.1038/s41396-021-01050-5>.
- Price, M.N., Dehal, P.S., Arkin, A.P., 2010. FastTree 2-approximately maximum-likelihood trees for large alignments. *PLoS One* 5, e9490. <https://doi.org/10.1371/journal.pone.0009490>.
- Ramsby, B.D., Hoogenboom, M.O., Whalan, S., Webster, N.S., 2018. Elevated seawater temperature disrupts the microbiome of an ecologically important bioeroding sponge. *Mol. Ecol.* 27, 2124–2137. <https://doi.org/10.1111/mec.14544>.
- Ribeiro, B., Padua, A., Barno, A., et al., 2020. Assessing skeleton and microbiome responses of a calcareous sponge under thermal and pH stresses. *ICES J. Mar. Sci.* 78, 855–866. <https://doi.org/10.1093/icesjms/fsaa231>.
- Ribes, M., Calvo, E., Movilla, J., et al., 2016. Restructuring of the sponge microbiome favors tolerance to ocean acidification. *Environ. Microbiol. Rep.* 8, 536–544. <https://doi.org/10.1111/1758-2229.12430>.
- Rognes, T., Flouri, T., Nichols, B., et al., 2016. VSEARCH: a versatile open source tool for metagenomics. *PeerJ* 4, e2584. <https://doi.org/10.7717/peerj.2584>.
- Sabine, C.L., Feely, R.A., Gruber, N., et al., 2004. The oceanic sink for anthropogenic CO₂. *Science* 305, 367–371. <https://doi.org/10.1126/science.1097403>.
- Sacristán-Soriano, O., Turon, X., Hill, M., 2020. Microbiome structure of ecologically important bioeroding sponges (family Clionaidae): the role of host phylogeny and environmental plasticity. *Coral Reefs* 39, 1285–1298. <https://doi.org/10.1007/s00338-020-01962-2>.
- Sato, Y., Ling, E.Y.S., Turavev, D., et al., 2017. Unraveling the microbial processes of black band disease in corals through integrated genomics. *Sci. Rep.* 7, 40455. <https://doi.org/10.1038/srep40455>.
- Schläppli, M.L., Weber, M., Mendola, D., et al., 2010. Heterogeneous oxygenation resulting from active and passive flow in two Mediterranean sponges, *Dysidea avara* and *Chondrosia reniformis*. *Limnol. Oceanogr.* 55, 1289–1300. <https://doi.org/10.4319/lo.2010.55.3.1289>.
- Schönberg, C.H.L., Fang, J.K.-H., Carballo, J.L., 2017. Bioeroding sponges and the future of coral reefs. In: Carballo, J.L., Bell, J.J. (Eds.), *Climate change, ocean acidification and sponges*. Springer, Cham, pp. 179–372. https://doi.org/10.1007/978-3-319-59008-0_7.
- Shannon, P., Markiel, A., Ozier, O., et al., 2003. Cytoscape: a software environment for integrated models of biomolecular interaction networks. *Genome Res.* 13, 2498–2504. <https://doi.org/10.1101/gr.1239303>.
- Simister, R., Taylor, M.W., Tsai, P., et al., 2012. Thermal stress responses in the bacterial biosphere of the Great Barrier Reef sponge, *Rhopaloeides odorabile*. *Environ. Microbiol.* 14, 3232–3246. <https://doi.org/10.1111/1462-2920.12010>.
- Stevenson, A., Archer, S.K., Schultz, J.A., et al., 2020. Warming and acidification threaten glass sponge *Aphrocallistes vastus* pumping and reef formation. *Sci. Rep.* 10, 8176. <https://doi.org/10.1038/s41598-020-65220-9>.
- Strand, R., Whalan, S., Webster, N.S., et al., 2017. The response of a boreal deep-sea sponge holobiont to acute thermal stress. *Sci. Rep.* 7, 1660. <https://doi.org/10.1038/s41598-017-01091-x>.
- Strohm, T.O., Griffin, B., Zumft, W.G., Schink, B., 2007. Growth yields in bacterial denitrification and nitrate ammonification. *Appl. Environ. Microbiol.* 73, 1420–1424. <https://doi.org/10.1128/AEM.02508-06>.
- Sunagawa, S., DeSantis, T.Z., Piceno, Y.M., et al., 2009. Bacterial diversity and white plague disease-associated community changes in the Caribbean coral *Montastraea faveolata*. *ISME J.* 3, 512–521. <https://doi.org/10.1038/ismej.2008.131>.
- Sweet, M., Bulling, M., Cerrano, C., 2015. A novel sponge disease caused by a consortium of micro-organisms. *Coral Reefs* 34, 871–883. <https://doi.org/10.1007/s00338-015-1284-0>.
- Thomas, T., Rusch, D., DeMaere, M.Z., et al., 2010. Functional genomic signatures of sponge bacteria reveal unique and shared features of symbiosis. *ISME J.* 4, 1557–1567. <https://doi.org/10.1038/ismej.2010.74>.

- Thomas, T., Moitinho-Silva, L., Lurgi, M., et al., 2016. Diversity, structure and convergent evolution of the global sponge microbiome. *Nat. Commun.* 7, 11870. <https://doi.org/10.1038/ncomms11870>.
- Tomich, M., Planet, P.J., Figurski, D.H., 2007. The *tad* locus: postcards from the widespread colonization island. *Nat. Rev. Microbiol* 5, 363–375. <https://doi.org/10.1038/nrmicro1636>.
- Turon, M., Caliz, J., Triado-Margarit, X., et al., 2019. Sponges and their microbiomes show similar community metrics across impacted and well-preserved reefs. *Front Microbiol* 10, 1961. <https://doi.org/10.3389/fmicb.2019.01961>.
- Ugarelli, K., Chakrabarti, S., Laas, P., Stingl, U., 2017. The seagrass holobiont and its microbiome. *Microorganisms* 5, 81. <https://doi.org/10.3390/microorganisms5040081>.
- Vargas, S., Leiva, L., Wörheide, G., 2021. Short-term exposure to high-temperature water causes a shift in the microbiome of the common aquarium sponge *Lendenfeldia chondrodes*. *Micro Ecol.* 81, 213–222. <https://doi.org/10.1007/s00248-020-01556-z>.
- Webster, N.S., Thomas, T., 2016. The sponge hologenome. *mBio* 7, e00135–16. <https://doi.org/10.1128/mBio.00135-16>.
- Webster, N.S., Botté, E.S., Soo, R.M., Whalan, S., 2011. The larval sponge holobiont exhibits high thermal tolerance. *Environ. Microbiol Rep.* 3, 756–762. <https://doi.org/10.1111/j.1758-2229.2011.00296.x>.
- Weisz, J.B., Lindquist, N., Martens, C.S., 2008. Do associated microbial abundances impact marine demosponge pumping rates and tissue densities. *Oecologia* 155, 367–376. <https://doi.org/10.1007/s00442-007-0910-0>.
- Welsh, R.M., Rosales, S.M., Zaneveld, J.R., et al., 2017. Alien vs. predator: bacterial challenge alters coral microbiomes unless controlled by *Halobacteriovorax* predators. *PeerJ* 5, e3315. <https://doi.org/10.7717/peerj.3315>.
- WMO, 2020. WMO Statement on the state of the global climate in 2019. WMO, Geneva, Switzerland. https://library.wmo.int/doc_num.php?explnum_id=10211.
- Wu, C.-F., Lin, J.-S., Shaw, G.-C., Lai, E.-M., 2012. Acid-induced type VI secretion system is regulated by ExoR-ChvG/ChvI signaling cascade in *Agrobacterium tumefaciens*. *PLoS Pathog.* 8, e1002938 <https://doi.org/10.1371/journal.ppat.1002938>.
- Yang, M.J., Xu, D., Yang, D.X., et al., 2020. Malate enhances survival of zebrafish against *Vibrio alginolyticus* infection in the same manner as taurine. *Virulence* 11, 349–364. <https://doi.org/10.1080/21505594.2020.1750123>.
- Zhao, H.T., Wang, L.R., Song, C.J., 2008. Existing and developing conditions of coral reef on the west Xuwen county. *Trop. Geo* 28, 234–241. <https://doi.org/10.3969/j.issn.1001-5221.2008.03.008>.